HYDROGENATION PROPERTIES OF $Gd_{1-x}Ti_xNi$ $(0 < x < 1)$

K. Kluziak[1], V. Pavlyuk[1,2] ID

[1]*Institute of Chemistry, Jan Długosz University in Częstochowa,*
13/15, Armii Krajowej al., Częstochowa, 42-200, Poland,
[2]*Department for Inorganic Chemistry, Ivan Franko National University of Lviv,*
6, Kyrylo & Mefodiy St., Lviv, UA-79005, Ukraine

Rare-earth based alloys are the most popular combinations for creating electrode materials for nickel–metal–hydride (NiMH) batteries. This paper presents the results of electrochemical hydrogenation of AB type alloys $Gd_{1-x}Ti_xNi$ $(0 < x < 1)$. Good hydrogen storage properties of rare-earth metals are known, thanks to the insertion of the third component in the form of titanium the kinetics of hydrogen sorption/desorption have been improved and corrosion resistance has been increased. The synthesized of $Gd_{1-x}Ti_xNi$ $(0 < x < 1)$ alloys were studied by various experimental techniques, such as XRD, SEM, EPMA, gas and electrochemical hydrogenations. The insertion of Ti had a significant impact on improving the stability of charge/discharge cycles, corrosion protection, and reducing production costs by reducing the amount of rare earth metals. As an element capable of absorbing hydrogen titanium tends to form a passive oxide in 6M KOH electrolyte, which prevents corrosion of the anode.

Key words: alloys, electrochemical hydrogenation, hydrides, NiMH batteries, electrode materials, corrosion.

I. INTRODUCTION

The ever-increasing demand for energy and the depletion of fossil fuels and crude oil are forcing the search for new alternative and more economical energy sources. Environmental protection and the development of energy-saving technologies are equally important. Recently, an increase in the production of electric vehicles and hybrid cars can be observed, in which batteries play a dominant role as energy storage and conversion devices [1,2]. In recent years, there has been significant development of NiMH (metal hydride) batteries. The main area of research are negative electrodes in these cells. The nicke–hydride cell has a similar structure to that of nickel–cadmium batteries; the main difference is that nickel–hydride batteries use hydrogen absorbed in a metal alloy, which is a positive material.

Compared to nickel–cadmium batteries, NiMH cells have many advantages. These include high energy density, high efficiency, environmentally friendly electrode materials, no electrolyte consumption during charge/discharge cycles, no memory effect [2–14]. Due to the growing interest in these cells, new materials are being sought for use as the anode in these batteries. Rare-earth elements have a variety of physical properties, which allows using them as functional materials; more and more often they are chosen as negative electrodes in hydrogen cells.

The most important features that the alloy should have to be used as an anode material in NiMH are: good corrosion resistance, adequate hydrogen balance (suitable hydrogen equilibrium), long service life, good electrochemical catalysis, low cost (including energy consumption), long life cycle, balance of potential and current density, as well as stability during storage at high temperatures [1,2,13]. The electrochemical behavior of such compounds depends on the structure, the type of phases, and the amount of elements in the intermetallic compound. These properties can be influenced by designing the composition of the hydrogen storage alloy in order to ensure the highest efficiency of NiMH batteries. The alloys occurring as electrode materials in hydrogen cells consist of two types of metal in different stoichiometry, i. e. elements A and B with positive and negative hydrogen affinity, respectively. Depending on the ratio of A to B, hydrogen storage alloys are mainly classified as AB_5 type alloys, AB_2 type alloys, AB_3 type alloys, and AB type alloys. With increasing energy demand, new intermetallic compounds are being developed. One of them is electrode materials based on AB group with competitive parameters for industrial applications. The first alloy of type AB used in NiMH batteries in early 1970s, Ti–Ni, became a popular subject of research due to the relatively low cost of production, fast activation, and the high hydrogen storage capacity [10,11,15]. Large groups of metallic compounds, metals and alloys have been tested for their use as electrodes in hydrogen cells; the most promising among them are alloys based on rare-earth metals and alloys based on titanium and zirconium [4,11].

II. EXPERIMENTAL PART

A. Synthesis

The group of alloys $Gd_{1-x}Ti_xNi$ $(1 < x < 0)$ was prepared from the following reagents: gadolinium (wirereel, cutinto small pieces, 99.9 at.% Sigma Aldrich), nickel (powder, 99.9 at.% Sigma Aldrich), titanium (wire,cutinto small pieces, 99.9 at.% Sigma Aldrich). The pieces of the pure metals with calculated stoichiometries were pressed into a tablet and afterward were melted by

arc melting under pure argon atmosphere.

For the analysis of the number of phases in the synthesized alloys, the TESCAN electron microscope equipped with an EDS/WDS X-ray microanalyser was used. The phases content of the alloys was determined by X-ray diffraction (XRD, RigakuMiniFlex 600).

Alloys	Main phase	Additional phase
GdNi	Gd — 51.1% Ni — 48.9%	Gd — 64.2% Ni — 35.8%
$Gd_{0.9}Ti_{0.1}Ni$	Gd — 50.1% Ti — 3.2% Ni — 46.7%	Gd — 43.5% Ti — 8.0% Ni — 48.5%
$Gd_{0.8}Ti_{0.2}Ni$	Gd — 44.9% Ti — 5.2% Ni — 49.8%	Gd — 42.8% Ti — 8.2% Ni — 48.9%
$Gd_{0.7}Ti_{0.3}Ni$	Gd — 43.6% Ti — 6.7% Ni — 49.8%	Gd — 33.6% Ti — 9.9% Ni — 56.5%
$Gd_{0.5}Ti_{0.5}Ni$	Gd — 42.2% Ti — 8.4% Ni — 49.2%	Gd — 7.9% Ti — 43.3% Ni — 48.8%
$Gd_{0.3}Ti_{0.7}Ni$	Gd — 21.7% Ti — 30.6% Ni — 47.7%	Gd — 4.6% Ti — 47.2% Ni — 48.2%
$Gd_{0.1}Ti_{0.9}Ni$	Gd — 0.8% Ti — 47.3% Ni — 51.9%	Gd — 3.7% Ti — 41.9% Ni — 54.4%
TiNi	Ti — 51.8% Ni — 48.2%	

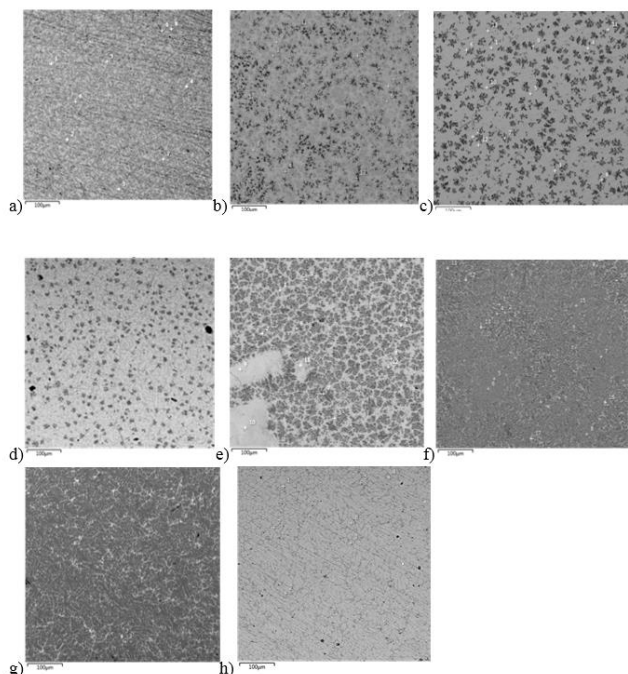Table 1. Percentage composition of individual elements (atomic %)

Fig. 1. The image from scanning electron microscope from a) GdNi, b) $Gd_{0.9}Ti_{0.1}Ni$, c) $Gd_{0.8}Ti_{0.2}Ni$, d) $Gd_{0.7}Ti_{0.3}Ni$, e) $Gd_{0.5}Ti_{0.5}Ni$, f) $Gd_{0.3}Ti_{0.7}Ni$, g) $Gd_{0.1}Ti_{0.9}Ni$, h) TiNi

B. Electrochemical hydrogeneration

Electrochemical analysis of all compounds was performed using potentiostat/galvanostat CH Instruments 600E (Austin, Texas, USA) and 8-channel BST8-MA battery analyzer (MTI Corporation, USA). Studies of the electrochemical characteristics were performed in SWAGELOK-type cells. Potentiokinetic polarization tests were carried out to characterize the corrosion resistance of the alloys tested. The electrochemical hydrogeneration was performed in two- and three-electrode SWAGELOK-type cells. The electrolyte in both cases was 6M KOH. The corrosive potential and cyclic voltammetry were measured in a standard three-electrode cell. The ZView software package (ScribnerAssociates, 2017) was used to create and analyze impedance charts.

C. Hydrogen gas sorption investigation

Sorption properties were tested using a gas sorption analyser IMI HIDEN ISOCHEMA. The analyser allows us to determine the amount of gas absorbed by the sample, under controlled pressure and temperature conditions, using the Siverts volumetric method. The kinetics of the sorption/desorption process as well as the durability of the material at cyclic absorption and desorption of gas within a specific range of temperature and pressure were investigated.

III. RESULTS AND DISCUSSION

A. Phase analysis

Figure 1 shows a list of images taken using SEM/EDS extension for group $Gd_{1-x}Ti_xNi$ alloys $(0 < x < 0)$. Scanning electron microscopy (SEM) confirms that the alloys have been properly synthesized in an appropriate mass ratio. The addition of titanium to the alloys as the third component decreased homogeneity. Table 1 shows the percentage compositions of individual elements occurring in each phase. For all alloys containing titanium, the formation of homogeneously distributed black dots is observed, in which the presence of the phase with the predominant proportion of titanium is revealed. X-ray analysis showed that in the synthesized samples the main phases are solid solutions based on binary compounds of GdNi and TiNi. The GdNi and TiNi phases crystallize in different structural types for this reason; between these phases limited solid solutions are formed. On the basis of the qualitative and quantitative phase analysis and EDS spectra analysis, it can be concluded that in the synthesized samples part of

Ti atoms (about 5%) is replaced with Gd atoms and vice versa. Diffractograms of $Gd_{1-x}Ti_xNi$ alloys are shown in Fig. 2; they show significant amorphousness of the synthesized samples. Figure 3 shows the region of homogeneity and extension of solid solutions $Gd_{1-x}Ti_xNi$ and $Ti_{1-x}Gd_xNi$, between which there is a two-phase equilibrium.
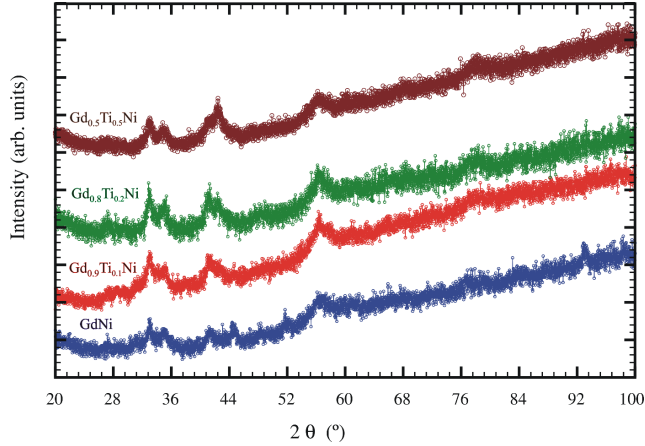
Fig. 2. Powder patterns for some alloys from $Gd_{1-x}Ti_xNi$ solid solution (GdNi, $Gd_{0.9}Ti_{0.1}Ni$, $Gd_{0.8}Ti_{0.2}Ni$, $Gd_{0.5}Ti_{0.5}Ni$)
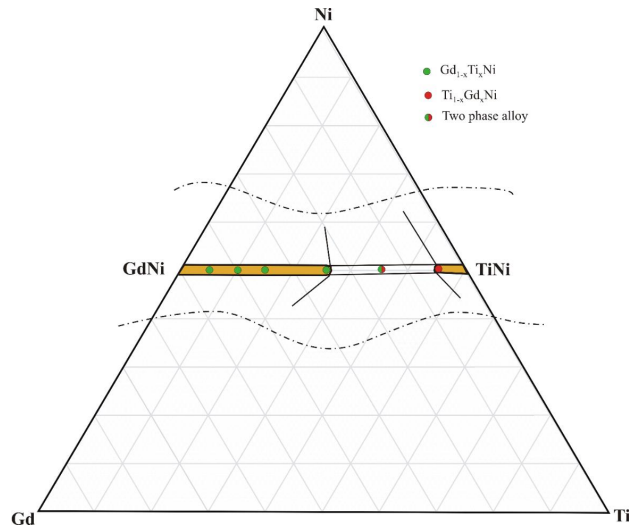
Fig. 3. The region of homogeneity and extension of $Gd_{1-x}T_xNi$ and $Ti_{1-x}Gd_xNi$ solid solutions

B.   Electrochemical hydrogenation

After the phase and structural analysis some samples of synthesized alloys were selected for electrochemical studies. The obtained alloys were tested in the battery prototype with a two-electrode cell consisting of an anode (alloy), electrolyte (6M KOH) and cathode (alkaline paste consisting of $Ni(OH)_2$ and graphite).
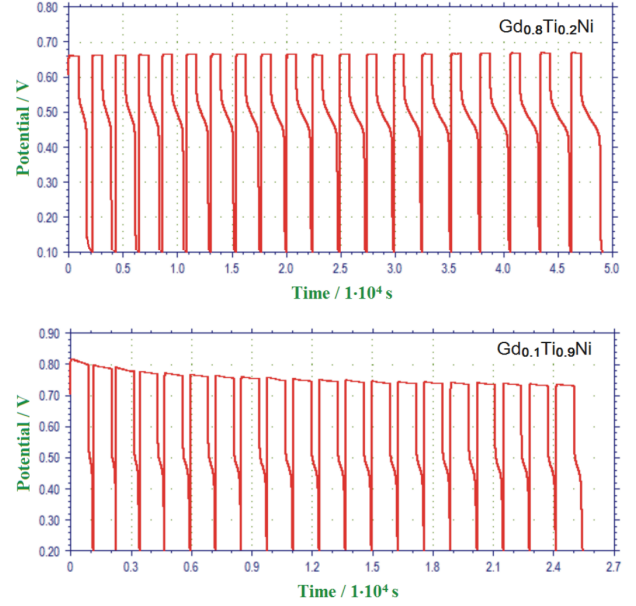

Fig. 4. Galvanostatic charge/discharge cycles for $Gd_{0.8}Ti_{0.2}Ni$ (top), $Gd_{0.1}Ti_{0.9}Ni$ (bottom)
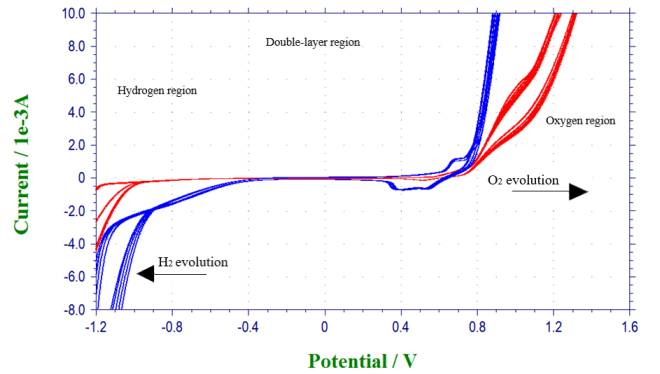
Fig. 5. (Color online). The cyclic voltammograms for $Gd_{0.8}Ti_{0.2}Ni$ (red), $Gd_{0.1}Ti_{0.9}Ni$ (blue)
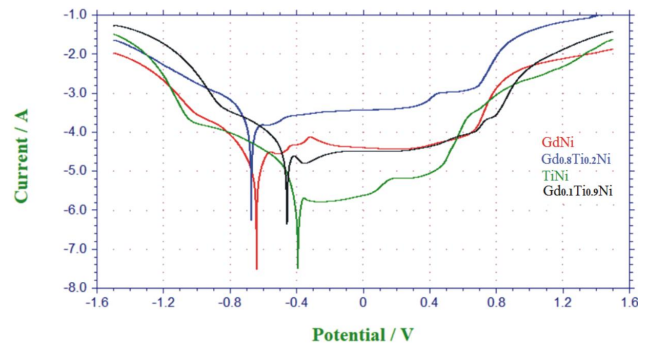

Fig. 6. (Color online). Potentiodynamic polarization curves for GdNi (red), $Gd_{0.8}Ti_{0.2}Ni$ (blue), TiNi (red), $Gd_{0.1}Ti_{0.9}Ni$ (blue)

Figure 4 shows the galvanostatic charging/discharging curves for $Gd_{0.8}Ti_{0.2}Ni$ and $Gd_{0.1}Ti_{0.9}Ni$ alloy electrodes in 6 M KOH, using the set value of the charging current ($i_{charge} = 2\,mA\,cm^{-2}$) and discharge ($i_{discharge} = 1\,mA\,cm^{-2}$), which indicate the good cycle stability of

both electrodes.

Figure 5 shows cyclic voltammogram (CV) curves of the $Gd_{0.8}Ti_{0.2}Ni$ and $Gd_{0.1}Ti_{0.9}Ni$ electrodes in the 6 M KOH solution. In the cathodic branch of the voltammogram, a change in the slope of the curve is observed at a potential around -1.0 V, which is probably associated with the adsorption of hydrogen atoms on the electrode surface.

The corrosion potential of the electrode (E_{corr}) for GdNi is -0.64 V, while for the alloy $Gd_{0.8}Ti_{0.2}Ni$ it is shifted to -0.68 V (Fig. 6). The situation is similar in the case of TiNi alloy, for which the corrosion potential is -0.39 V and for $Gd_{0.3}Ti_{0.7}Ni$ there is a shift to -0.46 V. The analysis of previous research showed that the addition of a small amount of titanium improves the corrosion resistance [5], which was confirmed by our research.
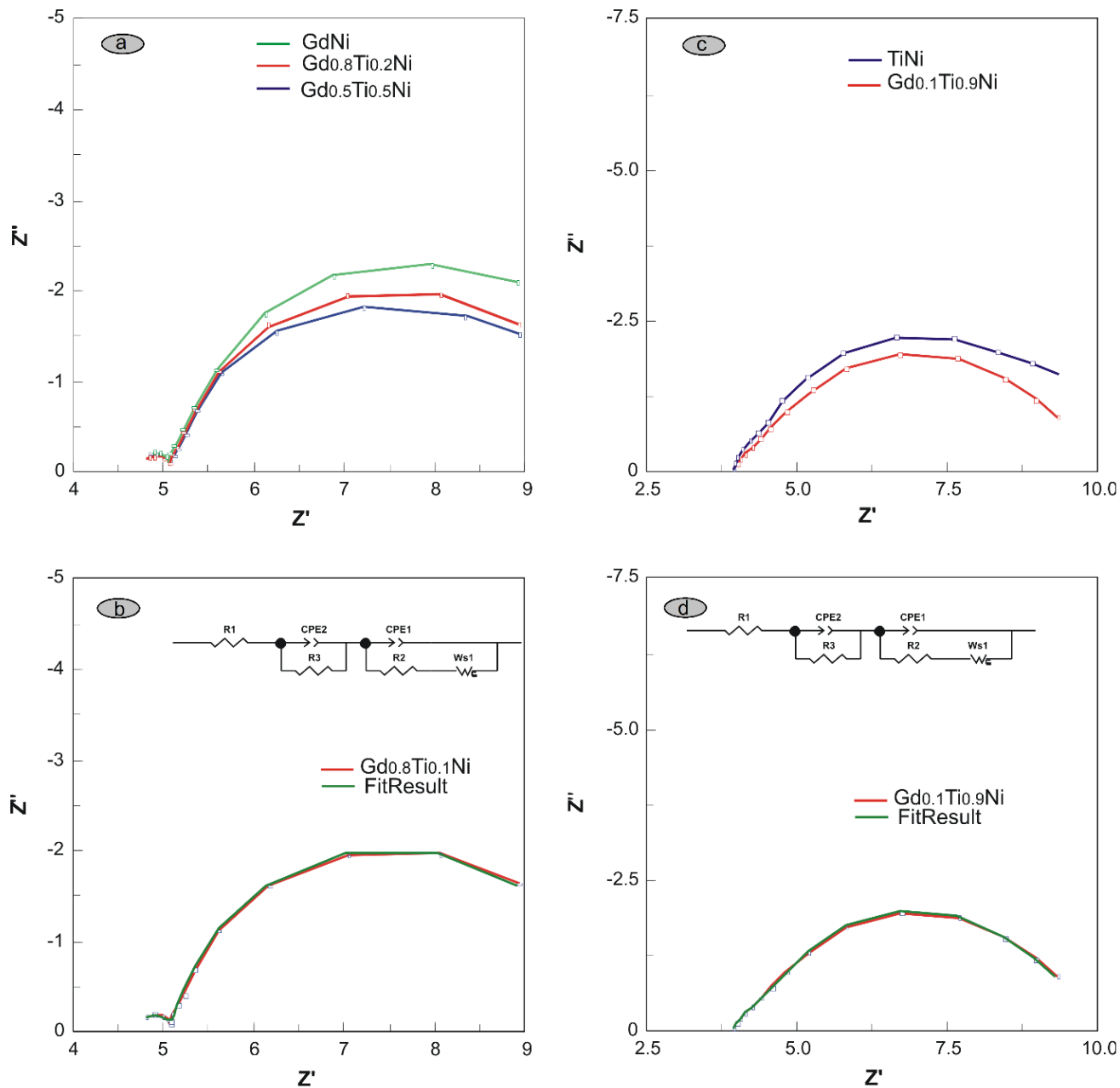

Fig. 7. EIS results for $Gd_{1-x}Ti_xNi$ (a), data analyzed by fitting to an equivalent electrical circuit (inset) for $Gd_{0.8}Ti_{0.2}Ni$ (b) and for $Ti_{1-x}Gd_xNi$ (c, d) electrodes in 6 M KOH solution

Figure 7 shows the electrochemical impedance spectra (EIS) of $Gd_{1-x}Ti_xNi$ and $Ti_{1-x}Gd_xNi$ alloy electrodes. The depressed semicircle is attributed to the charge transfer resistance (R_{ct}). For both solid solutions, as a result of the replacement with the third component, there is a decrease in the diameter of the semicircle, which indi-

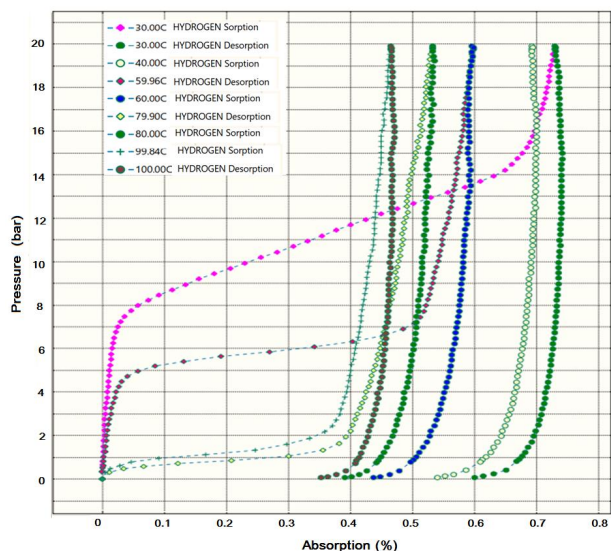cates that the charge transfer reaction is facilitated for the substituted alloy electrodes.

Fig. 8. Hydrogen sorption test for the $Gd_{1-x}Ti_xNi$ $(x = 0.1)$ alloy in temperature range 30–100°C
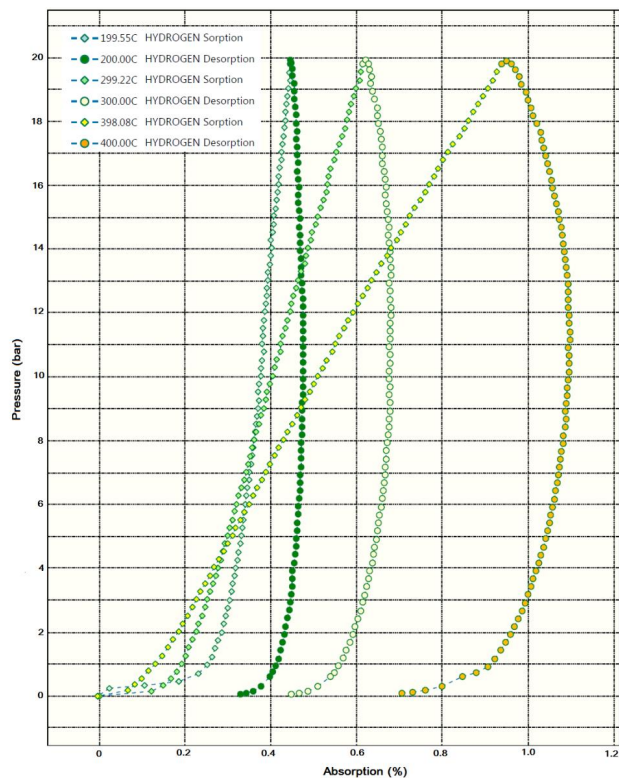

Fig. 9. Hydrogen sorption test for the $Gd_{1-x}Ti_xNi$ $(x = 0.1)$ alloy in temperature range 200–400°C
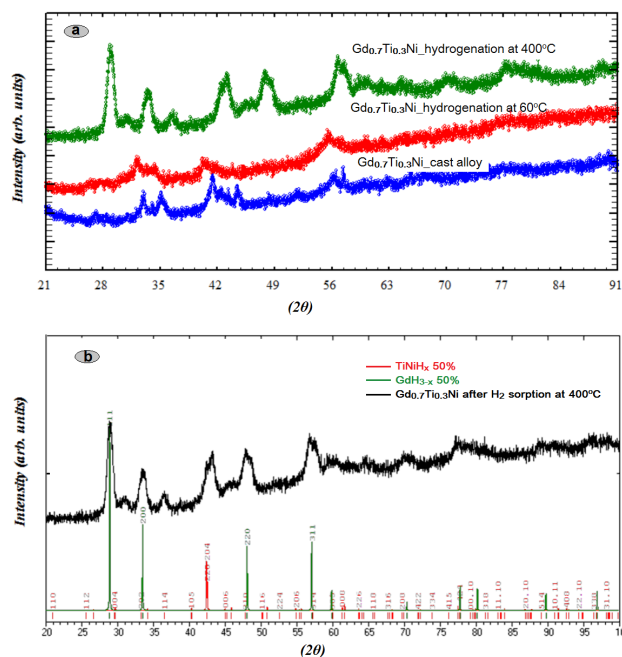

Fig. 10. Powder patterns for $Gd_{0.7}Ti_{0.3}Ni$ alloy and their hydrides
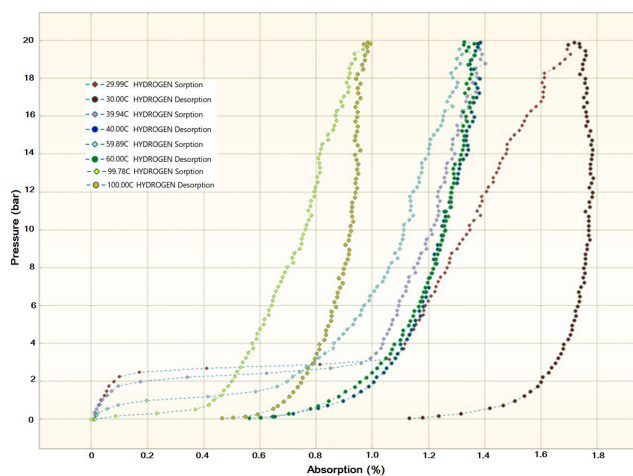

Fig. 11. Hydrogen sorption test for the $Ti_{1-x}Gd_xNi$ $(x = 0.1)$ alloy in temperature range 30–100°C

C. Gas phase hydrogenation

The PC isotherms of the hydrogen absorption/desorption for the both solid solution phases of $Gd_{1-x}Ti_xNi$ and $Ti_{1-x}Gd_xNi$ were measured in the temperature range from 30°C up to 400°C and the hydrogen pressure range from 0.01 to 20 bar. For the $Gd_{1-x}Ti_xNi$, phase the formation of cubic hydride phase in the temperature range up to 100°C was observed. The cubic hydride phase formed by insertion of hydrogen in the structure of the initial intermetallic phase. The

maximum solubility of hydrogen in $Gd_{1-x}Ti_xNi$ phase reached 0.7 wt.% (Fig. 8). At temperatures above 100°C, in addition to the cubic phase, a stable tetragonal phase is formed and the hydrogen content reaches 1.1 wt.% (Fig. 9).
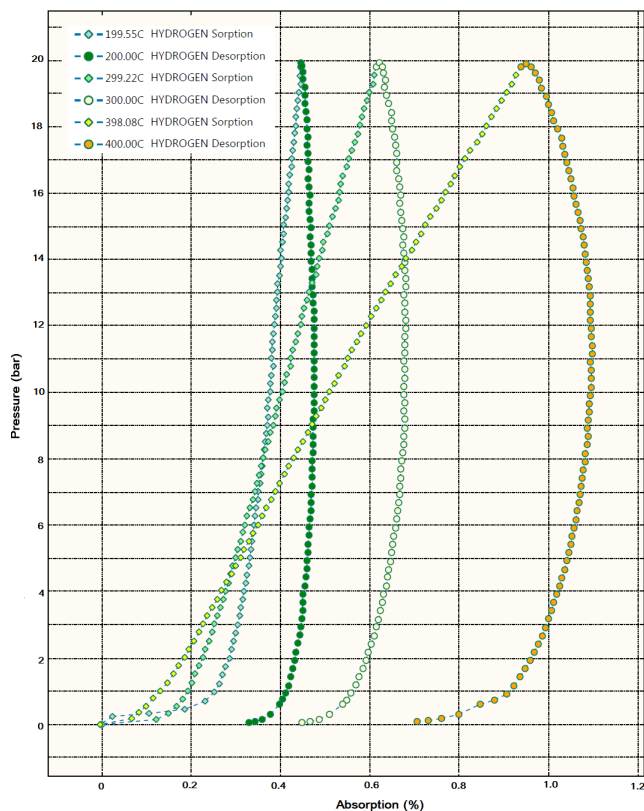

Fig. 12. Hydrogen sorption test for the $Ti_{1-x}Gd_xNi$ ($x = 0.1$) alloy in temperature range 200–400°C

After the sorption test, the powder diffractometer test was carried out again to check which part of the hydrogen remains in the alloy to form hydride. On the diffractograms of a hydrogenated sample, additional diffraction reflexes appear (at angles 29.5° and 39.0°) that belong to a new tetragonal hydride phase, which is more stable (Fig. 10). The absorption of hydrogen by the $Ti_{1-x}Gd_xNi$ alloy of the solid solution is much better, and in the temperature range up to 100°C the hydrogen capacity reaches 1.7 wt.% (Fig. 11). At temperatures above 100°C, the hydrogen capacity decreased and the equilibrium plateau disappeared (Fig. 12).

D. CONCLUSION

Our research showed that partial replacement of gadolinium atoms with titanium improves the electrochemical and sorption properties of this system. Moreover, a solid solution based on GdNi and TiNi is formed, which was confirmed by tests carried out using a powder diffractometer. Sorption tests for selected alloys were carried out in a wide temperature range. After analysis of their results, it can be seen that the reversibility of the absorption process is much better at lower temperatures. Diffractograms for hydrogenated samples (after sorption tests) show the formation of two new hydride phases, cubic $Gd_{1-x}Ti_xNiH_y$ ($0 < x < 0.2$) and tetragonal $Gd_{1-x}Ti_xNiH_y$ ($0.2 < x < 1.0$).

[1] Y. Zhang, Y. Li, H. Shang, Z. Yuan, T. Yang, S. Guo, J. Solid. State Electrochem. **21**, 1015 (2017); https://doi.org/10.1007/s10008-016-3455-5.

[2] H. S. Kim *et al.*, Metals Mater. Int. **14**, 497 (2008); https://doi.org/10.3365/met.mat.2008.08.497.

[3] S. M. Lee, H. Lee, J. H. Kim, P. S. Lee, J. Y. Lee, Metals Mater. Int., **7**, 181 (2001); https://doi.org/10.1007/BF03026958.

[4] I. Y. Zavalii, I. V. Saldan, Mater. Sci. **38**, 526 (2002); https://doi.org/10.1023/A:1022958515503.

[5] S. S. Han, N. H. Goo, W. T. Jeong, K. S. Lee, J. Power Sources **92**, 157 (2001); https://doi.org/10.1016/S0378-7753(00)00516-4.

[6] B. Hosni, C. Khaldi, O. ElKedim, N. Fenineche, J. Lamloumi, Int. J. Hydrog. Energy **42**, 1420 (2017); https://doi.org/10.1016/j.ijhydene.2016.04.032.

[7] K. Hong, J. Alloys Compd. **321**, 307 (2001); https://doi.org/10.1016/S0925-8388(01)00957-4.

[8] M. Tliha *et al.*, J. Solid State Electrochem. **18**, 577 (2014); https://doi.org/10.1007/s10008-013-2300-3.

[9] K. Young, J. Nei, Materials **6**, 4574 (2013); https://doi.org/10.3390/ma6104574.

[10] F. Feng, M. Geng, D. O. Northwood, Int. J. Hydrog. Energy **26**, 725 (2001); https://doi.org/10.1016/S0360-3199(00)00127-0.

[11] T. Nobuki, J.-C. Crivello, F. Cuevas, J.-M. Joubert, Int. J. Hydrog. Energy **44**, 10770 (2019); https://doi.org/10.1016/j.ijhydene.2019.02.203.

[12] F. Cheng, J. Liang, Z. Tao, J. Chen, Adv. Mater. **23**, 1695 (2011); https://doi.org/10.1002/adma.201003587.

[13] F. Feng, J. Han, M. Geng, D. O. Northwood, J. Electroanal. Chem. **487**, 111 (2000); https://doi.org/10.1016/S0022-0728(00)00167-4.

[14] K. Shinyama *et al.*, Res. Chem. Intermed. **32**, 419 (2006); https://doi.org/10.1163/156856706777973718.

[15] F. Cuevas, J-M. Joubert, M. Latroche, A. Percheron-Guégan, Appl. Phys. **A72**, 225 (2001); https://doi.org/10.1007/s003390100775.

ГІДРОГЕНСОРБЦІЙНІ ВЛАСТИВОСТІ $\mathbf{Gd_{1-x}Ti_xNi}$ $(0 < x < 1)$

К. Клюзяк[1], В. Павлюк[1,2]

[1]*Інститут хімії, Університет імені Яна Длуґоша в Ченстохові,*
алея Армії Крайової, 13/15, 42-200, Ченстохова, Польща,
[2]*Кафедра неорганічної хімії, Львівський національний університет імені Івана Франка,*
вул. Кирила і Мефодія, 6, 79005, Львів, Україна

Сплави на основі рідкоземельних металів важливі для створення електродних матеріалів для нікель-метал-гідридних батарей (NiMH). У цій роботі подано результати електрохімічного гідрування сплавів типу AB $Gd_{1-x}Ti_xNi$ $(0 < x < 1)$. Відомо, що бінарні сплави рідкісноземельних металів, леґовані третім компонентом, а саме: титаном, мають поліпшену кінетику сорбції/десорбції водню та підвищену корозійну стійкість. Синтезовані сплави $Gd_{1-x}Ti_xNi$ $(0 < x < 1)$ вивчали різними експериментальними методами, як-от: рентґенівська дифракція, електронна мікроскопія, спектральний мікропробний аналіз, газове та електрохімічне гідрування. Леґування сплавів титаном має значний вплив на підвищення стабільності циклів заряду/розряду та підвищення корозійної стійкості. Титан схильний утворювати пасивувальну оксидну плівку в електроліті (6M розчин KOH), яка запобігає корозії електрода.

Ключові слова: сплави, електрохімічне гідрування, гідриди, NiMH-батареї, електродні матеріали, корозія.